Binder Jetting as Complementary Technology to Metal Injection Molding?

Metal Binder Jetting (MBJ) is an additive process in which binder is introduced locally into metal powder layers. The generated green parts are then debindered and sintered. In contrast to beam-based additive processes, hard materials can also be processed and, in principle, higher volumes or large, complex components can be produced more economically.

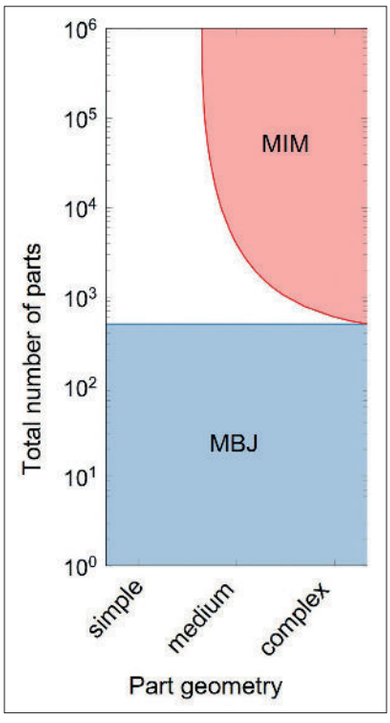

Fig. 1
Comparison between MBJ and MIM technology related to the total number and complexity of parts

Background

The process chain in MBJ is similar to that of Metal Injection Moulding (MIM), an established series production process in industry for complex components. However, MIM is uneconomical for small batches due to high tooling costs. The research institutes IWM at RWTH Aachen University and Fraunhofer IFAM are working together with a broad industrial consortium on achieving the MIM standard values for hardness, quasi-static tensile properties, and fatigue strength with optimised MBJ parameters and heat treatment of the steel AISI 630 (17-4PH®). However, a challenge for the industrial application of the MBJ process is the scattering of characteristic properties depending on the build space position and orientation, powder condition, and different MBJ equipment.

Keywords
metal binder jetting, metal injection moulding, mechanical properties, hardness, tensile testing, roughness, fatigue strength

Introduction

Metal Injection Moulding (MIM) is an established powder metallurgy process for complex shaped components in large-scale production. For prototype or small-scale production of powder metallurgical components with complex geometries in high quality, Additive Manufacturing (AM) processes are available. One AM process that has much in common with MIM is 3D printing using the metal binder jetting technology (MBJ). Fig. 1 evaluates the required number of pieces for an economic production of MIM and MBJ depending on the degree of complexity. MBJ technology fills the gap for small quantities that MIM leaves. Furthermore, MBJ has a higher production rate than beam-based AM Technologies such as powder-bed fusion – Laser Beam (PBF-LB) process or Powder Bed Fusion – Electron Beam (PBF-EB) process. [1]

In MBJ, a binder is selectively injected into a powder bed with a printhead. This is done layer by layer until the desired geometry is built. The part consisting of bonded powder particles is called green part. Green parts need to be removed from the powder bed, debindered and sintered. To ensure the reliable use of MBJ components and provide a suitable complement to MIM for small batches, some challenges have to be overcome first. Up to now, the process stability and the reproducibility are not ensured. Also, too little data is available for the mechanical performance of MBJ parts. Although several studies provide values for the tensile strength, yield strength, elongation and hardness of 316L [2, 3] and AISI 630® [4], investigations regarding the fatigue strength of MBJ parts is scarce. Data for 316L and IN625 are available [5, 6]. As comparison Marshal et al. [7] and Slaby et al. [8] could reach fatigue strength for MIM-AISI 630® of 415 MPa up to 470 MPa. In conventionally manufactured specimens made of AISI 630, fatigue strengths of up to 621 MPa could be achieved, depending on the grain size [9]. Increased porosity and the formation of silicon oxides are cited as causes for the lower fatigue strength of MIM AISI 630® parts [8].

F. Radtke, S. Herzog, S. Linnemann, C. Broeckmann
Institute for Materials Applications in Mechanical Engineering at RWTH Aachen University (IWM)
Aachen, Germany

E. Andreeva, C. Aumund-Kopp
Fraunhofer Institute for Manufacturing Technology and Advanced Materials (IFAM)
Bremen, Germany

Corresponding author: F. Radtke
E-mail: f.radtke@iwm.rwth-aachen.de

This study aims to answer the question which properties of MBJ components reach the minimum or typical MIM properties as defined in the MPIF standard 35 so far. These properties are determined on specimens from a first generation based on a lab-scale production and an up-scaled 2nd generation in small batch scale. The effect of post processing by hot isostatic pressing (HIP) to reduce porosity and anisotropy as well as different finished methods to decrease the surface roughness are discussed.

Material

The material used in this investigation, is a corrosion resistance and martensitic age hardening steel AISI 630 (1.4542, X5CrNiCuNb16-4, 17-4PH®). The chemical composition specified by the supplier is given in Tab. 1. A typical gas atomized, spherical AISI 630 MIM-powder, with an average nominal particle size D_{90} < 22 µm was used. The aim by working with MIM powder is to investigate, whether MIM manufacturers need to buy special binder jetting powders or work flexible with their existing MIM powders.

Specimen processing

The AISI 630 specimens were built in two different generation steps to optimise the process parameters and specimen geometries. The following Tab. 2 shows the used machine, layer thickness [µm], binder saturation [%], thermal debinding and sintering conditions, for the first and second process generation. 1st generation specimens were produced in many batches on an Innovent+ lab-scale machine while specimens of the 2nd generation were manufactured in one batch on a production machine 25 Pro.

Tab. 1
Chemical composition of the AISI 630 powder [mass-%]

C	Cr	Ni	Cu	Nb	Mo	Mn	O	N	Si	P	S	Fe
0,018	16,6	4,2	4,0	0,32	<0,03	0,54	0,06	<0,1	0,4	0,04	<0,01	Bal.

Tab. 2
Different binder jetting parameters of the 1st and 2nd generation

Binder Jetting Parameters	1st Generation	2nd Generation
Machine	ExOne Innovent+	ExOne X1 25Pro
Binder	In-house development	ExOne CleanFuse
Layer thickness [µm]	40	50
Binder saturation [%]	65	75
De-binding [°C/h]	1 h at 650 °C	1 h at 550 °C
Sintering [°C/h]	2 h at 1370 °C	3 h at 1320 °C

Due to an ultrasonic unit in the building chamber, a homogeneous distribution of the powder should be achieved in both generations. The printhead consists of many individual nozzles that print the binder to the desired locations. It moves continuously in x-direction, resulting in so-called binder-lines.

Thermal debinding and sintering was conducted in H_2 atmosphere. While the resulting porosity <5 vol.-% as determined by Archimedes method was the same in both generations, the higher sintering temperature in the 1st generation resulted in about 10 vol.-% delta-ferrite in the martensitic microstructure. After H900 heat treatment according to ASTM A564 a full martensitic microstructure was obtained in both generations. HIP (1150 °C , 100 MPa, 3 h) reduced the porosity observed in micrographs and the maximum pore diameter from 60 µm to 3 µm. Fig. 2 visualizes the process chain from metal powder to the component.

Achieved properties

Roughness and finishing methods

The roughness of MBJ specimens show significantly poorer results compared to conventionally manufactured components. The reason for this is the layer-by-layer build-up strategy. Different specimens were measured in this study using line profiles. While MIM components reach $Ra_{,MIM} = 1,0 \pm 0,2$ µm the average roughness of MBJ specimens amounts to $Ra_{,MBJ} = 3,3 \pm 0,3$ µm. The maximum peak to valley height Rz is three times higher ($Rz_{,MIM} = 4,8 \pm 1,1$ µm vs. $Rz_{,MBJ} = 16,1 \pm 1,3$ µm), too.

In the present study no improvement in surface roughness was obtained for specimens of the 2nd generation. In MBJ the layer thickness, the part orientation and the printing accuracy are crucial factors influencing the roughness.

For this reason, high productivity and low roughness play off each other. In addition to a poor optical impression, rough surfaces

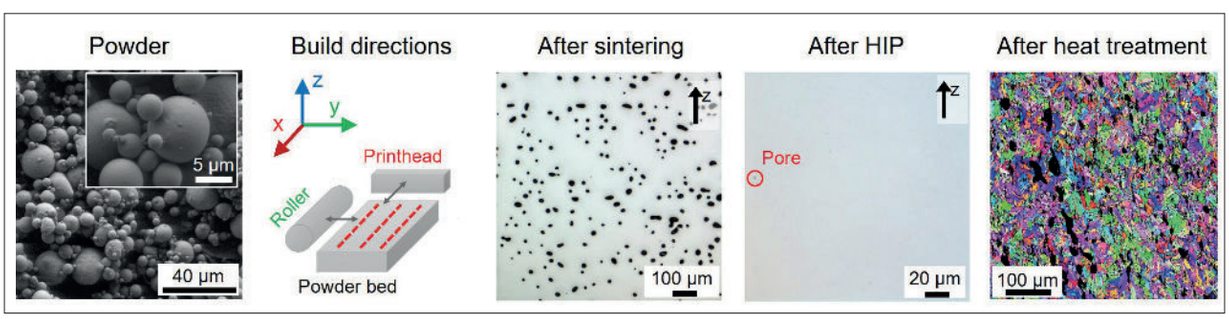

Fig. 2
Schematic figure of the specimen/microstructure evolution

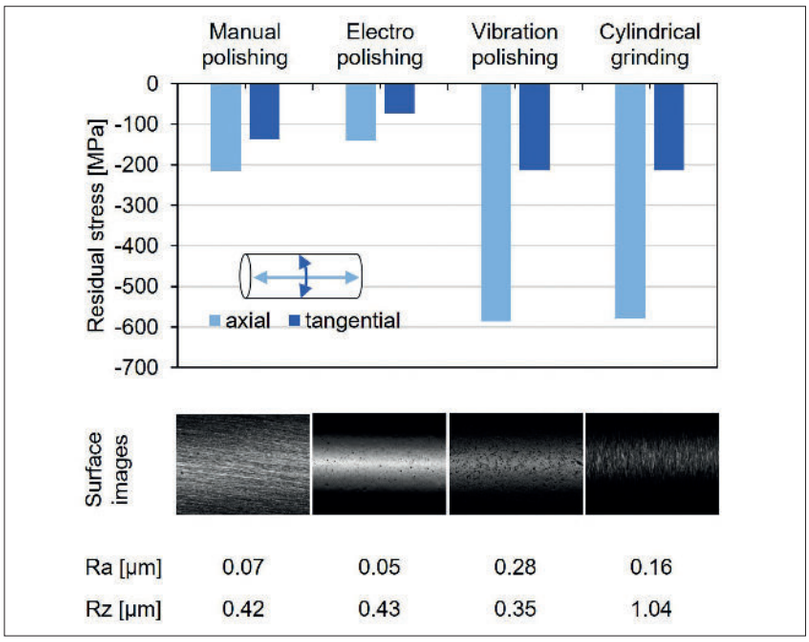

Fig. 3
Residual stress (average from 3 measurements), light optical images of and roughness obtained after finishing

also lead to a significant reduction in mechanical properties.

For the fatigue strength of dynamically stressed workpieces, the surface finish plays a special role, since fatigue cracks preferentially develop on the outer surface. Therefore, the fatigue strength is significantly determined by notches, surface roughness and inhomogeneities of the microstructure. To reduce the roughness of MBJ specimens and in order to characterise the influence of surface finishing on fatigue strength, we have used the following four surface finishing programs:

- Manual polishing
- Electro polishing
- Vibration finishing
- Cylindrical grinding with defined cutting edge.

These surface finishing programs are classified according to roughness and residual stresses. Residual stresses were measured using the X-ray diffraction (XRD) method. Results are summarised in Fig. 3. Manual polishing leads to very low Ra values, residual stresses between –100 and –200 MPa respectively and small grooves in tangential direction. In contrast to cylindrical grinding where grooves are in axial direction this is not crucial for fatigue strength. Cylindrical grinding and vibration polishing lead to very high compressive residual stresses. This is a positive side effect for components, but it biases the results of fatigue testing. Very smooth surfaces with visible pores and low residual stresses of –100 MPa are obtained after vibration polishing. With all finishing processes the roughness of the MIM specimens is exceeded by far.

All tested finishing methods enable to exceed the typical MIM roughness. In particular vibratory polishing is suitable as a simple and economical process for complex shaped components.

Tensile testing

Six different conditions, each with 10–20 specimen per generation were tested at room temperature on a Zwick/Roell ZMART Pro testing machine. The six specimen batches consist of two heat treatment conditions and each condition consists of specimens, built in the three different directions:

- Sintered (x-, y- and z-direction)
- Sintered + heat treated H900 (x-, y- and z-direction)
- Sintered + HIP + heat treated H900 (x-, y- and z-direction).

In Fig. 4 the results of the 1st generation of tensile test are shown, which were conducted on specimen, build up in different directions. From each series, half of the specimen were post densified by HIP before the heat treatment.

HIP leads to an improvement in yield strength and tensile strength. In the heat-treated condition the anisotropic nature is present in values of the ultimate tensile strength that decrease from x- via y- to z-direction. Even after post densification, the anisotropic behaviour persists. Unexpected were also the results in Yield strength val-

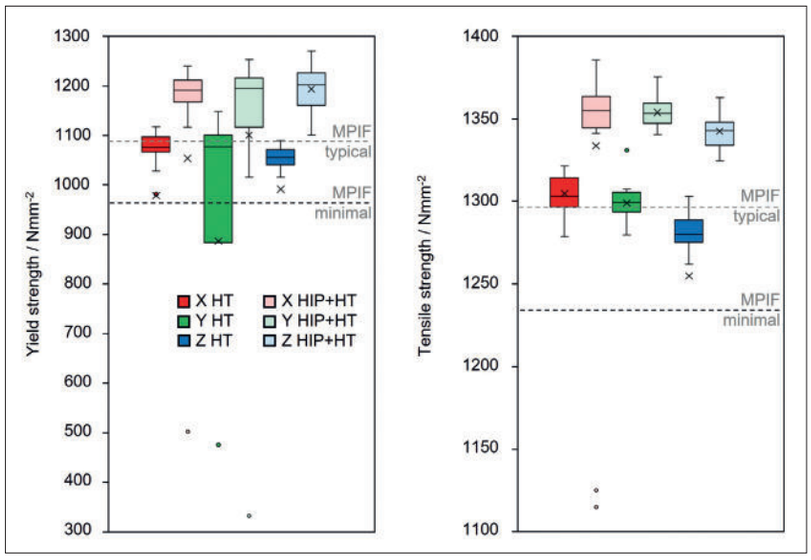

Fig. 4
Strength obtained in 1st generation in Heat-Treated Condition (HT) compared to the HIP + heat-treated condition (HIP+HT) shown as box-plots

Tab. 3
Mechanical properties of MBJ (1st and 2nd generation) and MIM Standard 35 values [11], mean values and standard deviation

Specimen Condition		R_m / N mm^{-2}	$R_{p0.2}$ / N mm^{-2}	At / %	HV10 / –
MBJ sintered + HT	1st	1191 ± 26	1078 ± 24	2–12	360
	2nd	1244 ± 19	888 ± 83	7 ± 1	355
MBJ sintered + HIP + HT	1st	1303 ± 23	1191 ± 47	–	–
	2nd	1364 ± 15	1098 ± 216	13,5 ± 1	–
MPIF 35 H900 minimal		1070	970	4	–
MPIF 35 H900 typical		1190	1090	6	330

ues. In y-direction a large scatter is observed in contrast to x and z direction for the heat-treated condition. Moreover, some outliers are found at a significantly lower level of yield strength, which could explain the high level of scatter. Even after HIP treatment, some of these protruding data points are still found, which can be attributed to incomplete HIP compaction. This leads to lower mechanical properties and increases the scatter level. A more constant scatter is present in the tensile strength values after HIP.

More or less all heat-treated specimens have values for yield strength and tensile strength that are between the minimum value and the typical MIM standard MPIF 35 [11]. HIP raises all values above the typical MPIF standard. The only exceptions are yield strength values obtained in y-direction and by some outliers in the x-direction.

After adjustment and scale-up of the MBJ process, specimens in 2nd generation were also tested. Tab. 3 compares the average values obtained in 1st and 2nd generation with the required standard of MIM specimens for AISI 630. The mean value of heat treated specimen in 1st and 2nd generation achieves the MPIF standard of 1190 N/mm² for the tensile strength. However, this is not the case for the yield strength. In general, the 2nd generation achieves a higher tensile strength and total elongation compared to the 1st generation. Typical MPIF values for tensile are achieved. HIP can increase the ductility for the second generation by a factor of 5, so that a value of 15 % could be achieved.

In the condition HIP+HT both generations can fulfil the MPIF standard. However, even for this condition, the 1st generation specimen has a higher value of more than 100 N/mm². HIP furthermore increases the ductility for the second generation by a factor of 5, so that a value of 14 % is achieved. The Standard hardness of MIM-17-4-PH of 330 HV10 can be exceeded after H900 heat-treated. Both generations are similar to each other, only a slight decrease can be seen in the second generation.

Overall, the second generation of specimens show a higher yield strength and elongation at fracture, but a slightly lower ultimate tensile strength and hardness.

Fatigue testing

Three different finishing methods with their characteristic compressive residual stresses were tested to evaluate the fatigue strength of the 2nd generation. The three groups were tested in the heat treated condition in two different building directions. Each group consists of 22–24 specimens in order to represent the distribution as accurate as possible.

- Manual polishing (x-direction, 22 specimens)
- Electro polishing (y-direction, 24 specimens)
- Vibration finishing (y-direction, 24 specimens).

S-N diagrams are prepared to determine the material and component-specific values under oscillating load (R = –1). For this purpose, the number of load cycles N are determined for different specimens on stress horizons at failure. The obtained S-N-curve describes the probability of failure at a certain number of cycles N for a given stress amplitude S. The stair-case method is used in this series of tests. Thereby, the stress amplitude applied depends on the previous specimen, so that the value settles to the mean value on its own. In addition, for the runouts (filled circles), the stress is raised to previously defined stress horizons to investigate the short-term strength of the specimens (triangles). The Dixon-Mood method was selected as the method to evaluate the 50 % long life fatigue. For high cycle fatigue, the Weibull distribution model was used. Both distribution models are included in SAFD 6 and were calculated with this software. The results of the fatigue tests represented as S-N-diagrams are given in Fig. 5.

The lowest fatigue strength with a value of 304 MPa is achieved by the vibration polished specimens built in y direction (blue). For the same building direction and finish-

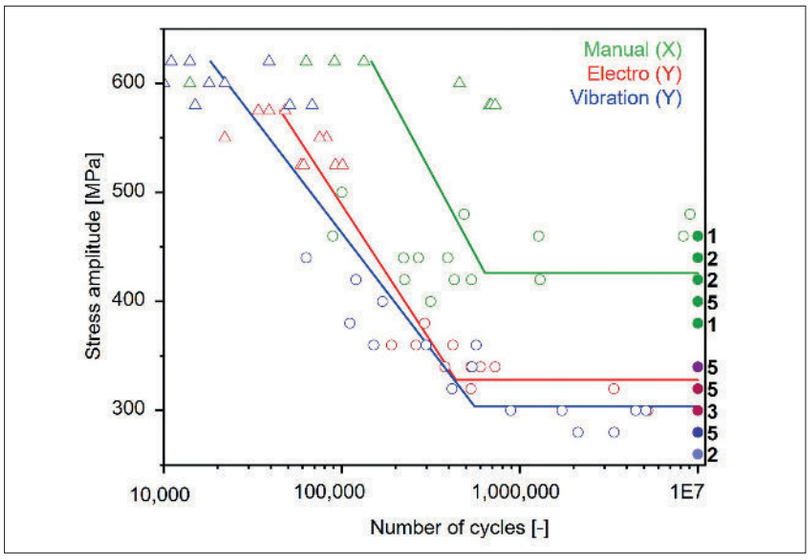

Fig. 5 S-N-diagrams for three tested groups of the 2nd generation. The fitted line represents 50 % fracture probability

Tab. 4
Fatigue strength results for three MBJ groups and two MIM references [7, 8]

Process	Polishing	Building Direction	R_z [µm]	Residual Stresses [MPa]	Fatigue Strength [MPa]
MBJ	Manual	X	0,42	–215	426 ± 45
MBJ	Electro	Y	0,43	–140	328 ± 30
MBJ	Vibration	Y	0,35	–586	304 ± 32
MIM	–	–	–		418–470 [7, 8]

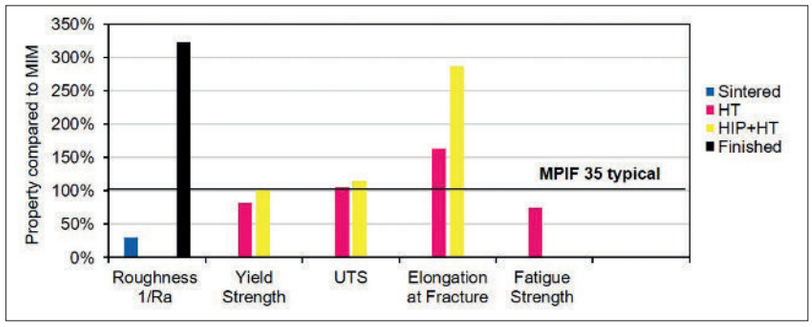

Fig. 6
Achieved properties of AISI 630 processed by MBJ compared to typical MIM values

ing by electro polishing a fatigue strength of 426 MPa can be achieved (red). Including the error values from Tab. 4, it can be seen that both fatigue strengths are almost identical. The residual stresses do obviously not influence the fatigue strength for MBJ specimens. Both S-N-lines fit well to the measured data points even for the high cycle fatigue as for the long life fatigue. The highest fatigue strength with a value of 426 MPa is present in manual polished specimens. However, the residual stresses for this polishing method lie between manual polishing and electro polishing.

The deviation of the S-N-line to the data points is strikingly poor. Also, the scattering in HCF and LLF is even higher compared to the other S-N-diagrams. A high overlap between up staired runouts and failed specimens at lower load cycles shows poor reproducibility of the results which can be detected in a higher error value in Tab. 4.

A reason for this problem lies in a bad reproducibility in manual machine using that always contains human error. Since no significant difference could be found within the roughness's, the only other difference between the specimens is the building production. The results in Fig. 5 and Tab. 4 show that the build direction of the specimen is more important than the residual stresses and the roughness of the specimens. As already explained is this caused in binder-lines, that appear along the x-direction. These binder-lines might cause lack of fusion of the metal powder particles and to a reduced green density. In addition, the nozzles of the machine may be clogged, which also increases the effect of the lower green density and an enrichment of pores along the binder lines.

This effects lead to a reduction of mechanical properties and lead to a anisotropic material behaviour [10].

For specimens printed along the y-direction a significantly higher number of binder lines can be detected and leads to decreased fatigue strength. The comparison to typical MIM values of AISI 630 in Tab. 4 shows that MBJ best case can reach the limits of MIM specimens.

Summary

To sum up all different properties, Fig. 6 compares the results of MBJ specimens in three different heat-treatment conditions with MIM values. The table supplies the averaged values over all directions x, y and z of the 2nd generation. The value 100 % property compared to MIM represents the MPIF Standard 35 values and some literature results for Fatigue strength of MIM-17-4-PH.

The roughness of sintered MBJ specimens cannot reach typical MIM values. All four tested finishing methods lead to a significant improvement of the roughness.

Typical MIM properties are achieved for UTS and fracture elongation. Regarding the yield strength as the most important property for mechanical designers, a HIP post-treatment is essential to reach the MIM standard. The middle value of the fatigue strength cannot be reached for sintered and heat-treated condition.

The results showed a highly anisotropic behaviour in addition to binder-lines for different specimen building directions. Further investigations including these phenomena should be performed. In addition, the condition of HIP plus heat-treated needs to be investigated. This could be an option to suppress the anisotropic fatigue strength for MBJ specimens.

To finalize the Question: Is Metal Binder Jetting a complementary technology to Metal Injection Moulding? Currently not yet! Due to process stability obtained with the used equipment and powders, a HIP post treatment was necessary to reach typical MIM typical properties. Further development will be necessary to reliably reach standard MIM properties.

Acknowledgement

This project was funded by the German Federation of Industrial Research Associations (AiF) under the contract number 21421. The authors thank Krämer Engineering, MIMplus Technologies, and OTEC Präzisionsfinish for their support in specimen finishing.

References

[1] Gokuldoss, P.K.; Kolla, S.; Eckert, J.: Additive manufacturing processes: Selective laser melting, electron beam melting and binder jetting-selection guidelines. In: Materials (Basel) **10** (2017) 6

[2] Barthel, B.; et al.: Influence of particle size distribution in metal binder jetting – effects on the properties of green and sintered parts. EuroPM 2019

[3] Mirzababaei, S.; Pasebani, S.: A review on binder jet additive manufacturing of

316L stainless steel. In: J. of Manufacturing and Mater. Processing **3** (2019) [3] 82
[4] Carreño-Morelli, E.; et al.: Three-dimensional printing of stainless steel parts. In: Mater. Sci. Forum **591–593** (2008) 374–379
[5] Schneider, M.; Hoeges, S.; Wawoczny, D.: Schwingfestigkeit des Stahls 316L – Vergleich zweier generativer Prozesserouten, Hagener Symposium, 2018
[6] Mostafaei, A.; et al.: Characterizing surface finish and fatigue behavior in binder-jet 3D-printed nickel-based superalloy 625. In: Additive Manufacturing **24** (2018) 200–209
[7] Marshall, T.P.: Injection molding of AISI 630 stainless steel **93** (1984) Section 6, 375–401
[8] Slaby, S.A.; Kraft, O.; Eberl, C.: Fatigue properties of conventionally manufactured and micro-powder-injection-moulded 17-4PH micro-components. In: Fatigue & Fracture of Engin. Mater. & Structures **39** (2016) [6] 780–789
[9] Aksteel: Data Sheet AISI 630
[10] Mostafaei, A.; et al.: Binder jet 3D printing – Process parameters, materials, properties, modeling, and challenges. In: Progress in Mater. Sci. **119** (2021) 100707
[11] MPIF: Materials standards for metal injection molded parts (2016). MPFI Standard 35